Interactions between alkali-activated ground granulated blastfurnace slag and organic matter in soil stabilization/solidification

Thomas Wattez, Cédric Patapy, Laurent Frouin, Julien Waligora, Martin Cyr

Interactions between alkali-activated ground granulated blastfurnace slag and organic matter in soil stabilization/solidification

Thomas Wattez [1], Cédric Patapy [1], Laurent Frouin [2], Julien Waligora [3], Martin Cyr [1]

(1) LMDC, Université de Toulouse, INSA, UPS, Génie Civil, 135 Avenue de Rangueil, 31077 Toulouse Cedex 04, France
(2) ECOCEM Materials, 4 place Louis Armand, 75012 Paris, France
(3) EIFFAGE Infrastructures, 8 Rue du Dauphiné, 69960 Corbas, France

Key words: stabilization/solidification; boring mud; alkali-activated slag; organic matter

Abstract

This paper presents novel findings regarding the use of alkali-activated slag for the development of road applications and, more particularly, how the interactions that occur between the binder and the organic matter originally present in the soil can strongly affect its reactivity in the process of stabilization and solidification. The study uses mechanical performances and macroscopic characterization, such as isothermal calorimetry and thermogravimetric analysis of the pure binders as well as of the soil-binder mixes in order to characterize the hydration mechanisms. By analyzing the chemical composition of organic matter extracted with three different alkaline activators, it is shown that both humic and fulvic acids are strong complexing agents, not only of calcium and aluminum ions, as noted in the existing scientific literature, but also of highly soluble silicon. In this study, only sodium hydroxide activated slag was found to be a suitable alkali-activated binder for subbase layer development.

1. Introduction

Civil Engineering projects have a tendency to generate large volumes of by-products and wastes during their realization. Tunnel boring is no exception and the muds extracted are rarely re-used in the vicinity of the work site but are more likely to be discarded in dedicated installations depending on the presence or absence of contaminants. For example, the current *Grand Paris* project intends to build about 200 kilometers of new metropolitan railway lines. This project is expected to produce about 45 million tons of tunnel boring muds. Finding sustainable solutions for dealing with such large volumes of materials was made an obligation by the French authorities at the birth of this project. Depending on the extraction sites, various contaminants can be encountered. They may be naturally occurring, such as sulfate [1-2] or molybdenum, or be present because, historically, heavy metals polluted unattended brownfield sites. The pollution levels indicate a need for evacuation and storage or, if possible, upcycling. This study, is particularly interested in the development of a subbase road layer where natural soil obtained from the tunnel boring process would be solidified over time with the addition of a cementitious binder.

Used instead of standardized sources of granular materials, the upcycling of waste to make subbase layers could lead to significant reduction of the CO_2 footprint in the area of road construction, through the implementation of circular economy initiatives. For example, previous work has shown the possibility of using dredged marine sediments for such applications [3,4]. Here, we considered using a tunnel boring mud extracted in the Paris region. The tunnel boring process implies that the retrieved material has a relatively high water content. In order to minimize post-processing steps, the waste soil was used here in its raw, highly humid state.

It can also be assumed that a significant part of the carbon footprint of a subbase layer comes from the binder used for its solidification, so the use of blended cements or clinker-free binders could lead to the CO_2 reduction sought. In particular, this work focused on evaluating the suitability of alkali-activated ground granulated blastfurnace slag for subbase layer development. Existing scientific literature shows promising results when alkali-activated materials, which have also been identified as geopolymers when the precursor consists solely of calcium-free, amorphous materials, are used for the stabilization and solidification of soils [5-14] that are potentially sulfated or polluted [15-18], with the final application to valorize them in road applications for example [19,20]. Yet, several limitations were noted in the scientific literature considerations and the conclusions drawn. To our knowledge, in the case of road subbase layer development, two factors are considered essential:

1) the early age compressive strength of the solidified soil. Essential to enable worksite trafficability and therefore project continuation, a minimal compressive strength of 1 MPa after 3 days of endogenous curing is key.

2) the economic viability of the selected binder. Apart from the lower environmental footprint of alkali-activated materials, their use must face economic competition. Binder dosage for soil treatment should not exceed a maximum of 10% by mass of dry soil, while using limited amounts of alkaline activator.

In these previous works, alkali-activated binder dosage with respect to the dry mass of the soil was set between 15% and 30% [7-9,11,15,19,20], which was not considered economically viable for this type of application. At the same time, activator concentration could reach extreme values such as 14M NaOH solutions [8,15,19] or even be added to amounts equivalent to the precursor, i.e. GGBS, metakaolin or fly ash, dosage [11,15]. Without exception, the earliest determined compressive strength was obtained after 7 days of endogenous curing. Even though they did not always reach the required minimal strength, alkali-activated binders were expected to provide suitable replacements for conventional binders such as OPC or quicklime. Additionally, for understandable reasons of material control, some studies [7,17] replaced natural soil by pure commercial clays, thus suppressing all interactions between the binder and the entire family of soil components such as non-clay minerals, soluble chemicals, organic matter, the only exception being the clay-binder reaction.

One key interaction was not taken into account in previous works regarding the use of alkali-activated binders for natural soil stabilization/solidification. It is common practice in geochemistry [21,22] to extract organic matter, and particularly leachable humic substances, by mixing alkaline solutions, often based on sodium hydroxide. The resulting supernatant solution displays a color varying between light yellow and dark brown, associated with both humic and fulvic acids. Because of their molecular structure, these species are known to be strong complexing agents of calcium and aluminum and therefore potential retarders of cementitious binders. Though recent discussions in the scientific literature [23] have pointed out the limitations of humic substance extraction based on alkaline solutions, the present study limited its description and findings to common knowledge and to protocol described in the literature and here below.

To ensure plausible comparison and analysis, three alkali-activated ground granulated blastfurnace slag binders were compared with two conventional binders, one being OPC and the other Slag-rich blended cement. Considering the differences in solidification reactivities observed through mechanical performance measurements, several analyses of the soil-binder matrix (isothermal calorimetry, thermogravimetric analysis, pore solution extraction) and the soil-alkaline solution interactions (organic matter extraction and precipitation) were carried out in this study.

2. Materials

2.1. Soil

The soil of interest in this study was a tunnel boring mud extracted from the south-western subsoil of a Paris suburb during the construction of a metro line. Characterizations of the soil consisted of the following measurements:

- Mineralogical composition by means of XRD test using a Bruker D8 advance diffractometer based on Cu-Kα radiation source (Fig. 1).
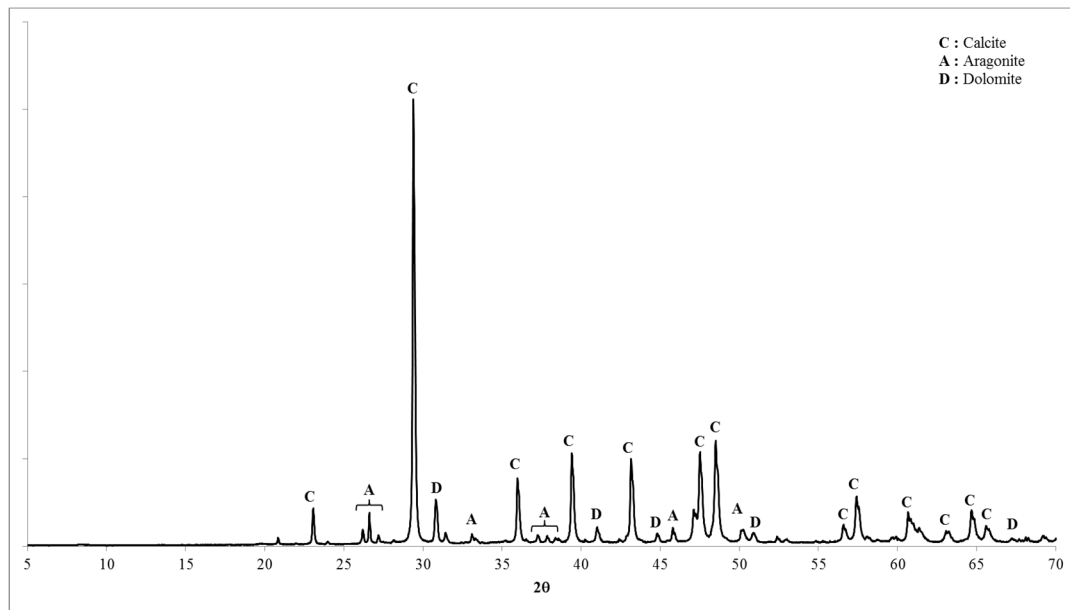

Figure 1 – XRD pattern of the soil.

The soil consisted mainly of carbonate-based mineralogical phases such as calcite, aragonite and dolomite. Remaining unidentified peaks in Fig. 1 were associated with traces of quartz. None of the sulfate minerals often expected in Paris underground types of soil [1] were reported for this material.

- Atterberg limits, Plastic and Liquid limits, were determined on granular fractions smaller than 400 µm and according to the French standard NF P94-051 [24]. A methylene blue absorption test (VBS), which relates to the clay content of the soil, was carried out on the granular fraction smaller than 5 mm, following NF P94-068 [25]. Initial water content of the soil was measured by drying approximately 500 grams of material at 105 °C until constant mass was reached. Total Organic Carbon (TOC) content was measured according to French standard XP P 94-047 [26] by calcining 300 grams of 5 mm sieved soil at a temperature of 475 °C for three hours.

The results for these five properties are summarized in Table 1.

Table 1 –Main soil properties determined

Properties	Value
Initial water content	25%
Plastic Limit	24%

Liquid Limit	30%
VBS	0.8
TOC	1.6%

Chemical composition of the mud was determined using ICP OES (Optima 7000DV – Perkin Elmer). The results are given in Table 2.

2.2. CEM I and GGBS

Ordinary Portland Cement (OPC) was provided by Vicat and fell within the category of CEM I 52.5N according to the French standard NF EN 197-1 [27]. Density and Blaine fineness were determined, giving values of 3.17 g/cm^3 and 4300 cm^2/g respectively. Ground Granulated Blastfurnace Slag (GGBS) was provided by Ecocem France. Its density and Blaine fineness were measured at values of 2.90 g/cm^3 and 4500 cm^2/g respectively.

Raw material chemical compositions were determined using ICP OES (Optima 7000DV - Perkin Elmer) and are summarized in Table 2.

Table 2 – Soil, Ordinary Portland Cement and Ground Granulated Blastfurnace Slag chemical compositions.

	Mass (%)										
	SiO_2	Al_2O_3	CaO	Fe_2O_3	MgO	TiO_2	SO_3	Cr_2O_3	Mn_2O_3	Na_2O_{eq}	LOI (%)
Mud	6.8	1.3	47.6	0.9	3.2	< 0.1	0.4	< 0.1	< 0.1	0.3	40.6
CEM I	19.9	3.9	64.0	4.5	2.5	0.2	2.1	N.D.	N.D.	0.4	1.1
GGBS	37.7	10.2	43.8	0.6	6.4	0.7	0.1	N.D.	N.D.	0.4	< 1.5

2.3. Alkaline activators

In this study, three types of alkaline activators were used: sodium hydroxide (NaOH), sodium metasilicate (Na_2SiO_3) and sodium carbonate (Na_2CO_3). All products were used in their powder form and were of analytical grade (purity > 99%).

3. Methods

3.1. Sample preparation

Stabilized mud samples were prepared by mixing the wet soil with up to five different types of binders. The masses given in Table 3 were designed for the fabrication of three prismatic samples (dimensions 4 cm x 4 cm x 16 cm) of stabilized mud. Two conventional binders, one based on 100% OPC (CEM I) and a slag-rich binder (CEM III/C), were compared with three alkali-activated slag based binders, one with sodium hydroxide (AAS-OH), one with sodium metasilicate (AAS-SiO) and one with sodium carbonate (AAS-CO).

Table 3 – Stabilized soil mixtures mass composition to prepare three prismatic samples.

	Mass (g)						
Name	Mud	CEM I	GGBS	NaOH	Na_2SiO_3	Na_2CO_3	Added Water
CEM I	1500	120					120

CEM III/C	1500	12	108				120
AAS-OH	1500		120	9.6			96
AAS-SiO	1500		120		14.7		96
AAS-CO	1500		120			12.0	72

The proportion of binder (CEM I or GGBS or mixture of the two) with respect to the dry mass of soil was set at 10%. Proportions of alkaline activators were selected in order to obtain a constant Na_2O_{eq} value of 6% in all the alkali-activated slag mixes.

Mixing was performed with a standard mortar mixer using the following protocol:

1. Chosen amount of wet mud, binders (CEM I and/or GGBS) and activators (NaOH, Na_2SiO_3, Na_2CO_3) were added to the mixing bowl.
2. The semi-dry content was mixed at low speed for up to three minutes.
3. Water was added in order to obtain a mix with a rheology allowing it to be cast in the prismatic molds afterwards.
4. The humidified blend of mud and binder was mixed at low speed for one minute then at high speed for an additional minute.

For all five binders studied, the resulting final mixture had a water content above 30%, which was significantly higher than the optimum moisture content of the treated soil. The mud-binder mixture was finally cast in two layers in the prismatic molds using a vibrating table. Samples were stored in sealed bags at 20 °C until tested.

3.2. Unconfined compressive strength

In order to evaluate the solidifying ability of a given binder for the type of soil, mechanical resistances of samples were determined through time. Unconfined compressive strength (UCS) measurements of stabilized mud samples were performed on prismatic samples cast beforehand and after four different curing durations: 3, 7, 28 and 60 days. For each curing time, three measurements were made on one prismatic sample. The loading rate was kept constant for all the tests at a value of 0.4 kN/s. Results summarized in Table 4 are given in terms of average value for the three measurements plus or minus the standard deviation.

3.3. Isothermal calorimetry

In order to assess the reactivity differences between the five binders of interest when used in the treatment of the calcareous soil, isothermal calorimetry measurements were made. For isothermal calorimetry testing, performed using a TAMair setup, samples were prepared as described below. The mud was first sieved at 10 mm in order for the mixture to fit within the testing bottles. For each mix design, 100 grams of mixture was prepared following the proportions given in Table 3 and keeping the total water content constant. Then, 10 grams of the freshly prepared batch was introduced into the testing bottle. Two bottles of each mix design were placed in the calorimeter. The test took place at a constant temperature of 20 °C and for 7 days.

3.4. In-situ pH

As a first explanation for binder-mud mixes reactivity (or lack thereof), in-situ pH values of freshly mixed stabilized samples were determined using a HACH Sension+ PH1 apparatus connected to a reinforced probe. One prismatic sample each of CEM III/C, AAS-SiO and AAS-CO were prepared following the proportions given in Table 3. Immediately after mixing, in-situ pH was determined by inserting the probe inside the batch. In between measurements, samples were stored in

sealed bags. Measurements stopped when setting occurred and the probe could no longer be safely inserted into the sample.

3.5. Pore solution extraction

To thoroughly evaluate the reactivity of conventional and alkali-activated binders when used in soil S/S, pore solution extractions were performed on additional stabilized mud samples. All types of binders were evaluated except the sodium carbonate activated GGBS (because of its lack of strength development with time). Extractions were performed on samples cured for 3, 7 and 28 days. Curing took place in endogenous conditions as for unconfined compressive strength testing. The apparatus and protocol employed to perform such extractions have been described by Cyr et al. [28]. At the end of the selected curing periods, samples were taken out of the sealed bags and crushed into centimetric fragments with a hammer, or by hand if their compressive strength was very low. Fragments were placed in a cylindrical metallic chamber that was sprayed with a thin layer of Teflon beforehand, to limit friction between fragments and the chamber walls. Pore solution was extracted by applying an axial load with a hydraulic press at a loading rate of 1 MPa/s, during which the maximum applied strength never exceeded 250 MPa. Pore solution was collected at the bottom of the cylindrical chamber in a polypropylene tube. Due to the mix design of stabilized mud samples and the high water content, between 15 and 20 mL of pore solution was obtained at every attempt. Immediately after extraction, the pH of the solution was measured with an LPH430T pH-meter. The solution was then filtered at 0.45 µm and acidified by adding 2% of nitric acid to avoid precipitation of species. Liquid samples were stored at 5 °C until the chemical composition was determined by ICP OES.

3.6. TGA

Alkali-activated binder reactivity was assessed through thermogravimetric analyses, performed using a Metler Toledo TGA 2 apparatus. The protocol followed a temperature ramp up of 5 °C per minute between 20 °C and 1000 °C. The testing atmosphere was exclusively argon gas. Before they were placed in the TGA chamber, hydration of the samples was stopped at the curing time of choice using a solvent exchange method, as described in [29], then ground in an agate mortar until 100% of the material was sieved at 80 µm. Only the sodium hydroxide and the sodium silicate activated binders were studied with this technique. In this case, pure samples of binder paste, with a water to GGBS ratio set to one, were prepared and cured (endogenous) for 3, 7 and 28 days. For comparison, stabilized soil samples with identical alkali-activated binders were prepared, always following the proportions given in Table 3, and cured for the same durations.

3.7. Organic matter extraction and precipitation

As pointed out earlier, mixing a natural soil and an alkaline source breaks down the clay-humus complex and releases humic substances into the liquid phase [22]. As this study focused on alkali-activated binders, organic matter, i.e. humic and fulvic acids, were extracted, separated and purified for analysis. First, organic matter was extracted from the raw soil by adapting the protocol described in the French standard NF EN 1744-1 [30]. The soil was first sieved at 16 mm and the non-passing fraction of the soil was coarsely crushed in order to also be sieved at 16 mm. In a 250 mL bottle, one third of the volume was filled with the sieved soil, and the remaining two thirds with an alkaline solution. The mix was shaken by hand for at least one minute and left to rest for 24 hours. The supernatant solution was finally filtered using 0.45 µm cellulose based Sartorius syringe filters in order to ensure that all small particles were eliminated. The French standard requires the exclusive use of a 3% (by mass) NaOH alkaline solution for the organic acids extraction. As for the alkali-activated

binders prepared for soil stabilization (Table 3), we also performed organic matter extraction with 4% (by mass) Na_2CO_3 and 4.6% (by mass) Na_2SiO_3 solutions. Alkaline solution concentrations were chosen in order to work at constant Na_2O_{eq}.

After filtering, the pH value of each supernatant solution was determined using the same apparatus as for in-situ measurements (3.4). Such solutions were considered to be mixtures of both fulvic and humic acids. The following protocol steps were designed to selectively precipitate each of the organic compounds. As described in [31], precipitation of humic acids after extraction in a highly alkaline environment was carried out by adding 4% by mass of pure nitric acid (HNO_3) so that the supernatant solution reached a pH value of 1. Pure acid addition was performed under constant stirring. The solution was left to settle for at least 24 hours. A thicker, darker phase, corresponding to precipitated humic acid, settled at the bottom of the sampling tube. The two phases were then separated. The residue was washed with distilled water until neutral pH was reached, avoiding sodium carbonate formation, and finally dried at 40 °C until constant mass was reached. , Assuming that the filtered solution contained exclusively fulvic acids, 2% by mass of aluminum chloride ($AlCl_3$) in its anhydrous powder form and 1% by mass of sodium hydroxide were added to it, both under constant stirring. Again, after 24 hours of settling, the thicker residue was filtered and washed with distilled water before being dried at 80 °C to constant mass. Due to the lack of resulting material, no analyses were performed on humic acid extracted with the 3% NaOH solution.

3.8. FTIR

In order to qualify the different types of humic substances extracted with the three alkaline solutions, Fourier Transform Infrared Spectroscopy (FTIR) measurements were performed on organic matter precipitates, both humic and fulvic acids, obtained after applying the protocol described in 3.7. A Perkin-Elmer apparatus functioning in the 4000 to 600 cm^{-1} wavenumber range was employed for this analysis.

3.9. Folin-Lowry method

To quantify the humic acid concentrations in the different solutions extracted when using the three alkaline activators, the modified Folin-Lowry method was used [31-35]. This method is based on reactivity differences of protein molecules and polyphenol-carrying molecules in alkaline conditions [34]. To highlight these differences, the solution to be evaluated was subjected to the protocol given below:

- 100 mL of Reagent A (RA) was prepared, consisting of 49 mL of a 5% Na_2CO_3 solution, 49 mL of a 0.2 M NaOH solution, 1 mL of a 2% $KNaC_4H_4O_6$ solution and 1 mL of a 1% $CuSO_4$ solution.
- 100 mL of Reagent B (RB) was prepared, consisting of the same mix as described for Reagent A but with the copper sulfate solution replaced by the same volume of distilled water.
- 40 µL of the sample was mixed with 200 µL of Reagent A.
- 40 µL of the sample was mixed with 200 µL of Reagent B.
- Calibration standards for both humic acids and proteins were prepared by diluting commercially available humic acid solutions (1 g/L) and bovine albumin solution (2 g/L) in distilled water. A total of six concentrations were used for the calibration curves, with a range set between 0 g/L (blanks) and 1 g/L. For each calibrating species and range, 40 µL of solution at the selected concentration was mixed with 200 µL of one of the reagents (A or B).

- After an incubation period of 10 minutes, 20 µL of the Folin-Ciocalteu reagent, an acid solution that is a mixture of phosphomolybdate and phosphotungstate, was added to each batch prepared in the previous steps.
- Additional incubation period of 30 minutes was followed.

In the case of the batches prepared with Reagent A, copper was expected to preferentially react with nitrogen atoms contained in the protein molecules [32,33]. The addition of the Folin-Ciocalteu reagent led to the second reduction of copper ions and the apparition of a blue colored solution. In the case of batches prepared with Reagent B, copper was not initially introduced and therefore the Folin-Ciocalteu acid reacted with the polyphenol molecules to give the blue color to the solution [32,35].

Concentrations in humic acid and protein were determined by measuring solution absorbance at a fixed wavelength of 750 nm using a FLUO star OPTIMA spectrometer. The specific absorbance of each compound of interest was determined through the following two equations [33]:

$$A_{total} = A_{sample,RA} - A_{blank,RA} = A_{protein} + A_{HA} \qquad (1)$$

$$A_{blind} = A_{sample,RB} - A_{blank,RB} = 0.2 \times A_{protein} + A_{HA} \qquad (2)$$

where A_{total} is the absolute absorbance measured in the sample mixed with reagent A (absorbance effectively measured minus blank absorbance), A_{blind} is the absolute absorbance measured in the sample mixed with reagent B, $A_{protein}$ is the absorbance associated with proteins potentially contained in the sample, A_{HA} is the absorbance associated with humic acid molecules potentially contained in the sample.

From these first two equations, absolute absorbance of both proteins and humic acid molecules was calculated in the following forms:

$$A_{protein} = 1.25 \times (A_{total} - A_{blind}) \qquad (3)$$

$$A_{HA} = 1.25 \times (A_{blind} - 0.2 \times A_{total}) \qquad (4)$$

From the initial calibration curves, for humic acid and animal protein (bovine albumin here), concentrations were obtained from the absorbance values calculated in equations (3) and (4).

3.10. Scanning Electron Microscopy

Scanning electron microscopy (SEM) images of precipitated organic compounds were obtained using a JEOL JSM-7200F apparatus in backscattered electron mode (energy varied between 5 and 15 keV) coupled with an EDS detector for elemental composition determination.

4. Results: soil-binder reactivity

This part summarizes the results regarding the soil-binder mixture reactivities. All five binders of interest were evaluated in terms of mechanical performance development over time, isothermal calorimetry measurements, in-situ pH values, pore solution extractions and compositions, and eventually thermogravimetric analysis.

4.1. Unconfined compressive strength

Unconfined compressive strengths obtained on prismatic samples of stabilized soil after four curing durations are summarized in Table 4. Among the five binders tested, the sodium hydroxide

activated slag (AAS-OH) produced the most suitable performances with respect to the targeted application, producing an early strength (3 days' curing) above 1 MPa and the second highest compressive strength after 60 days, close to 9 MPa.

Table 4 – Compressive strength evolution for the soil stabilized with the five different binders.

	Unconfined compressive strengths (MPa)			
Name	3 days	7 days	28 days	60 days
CEM I	1.6 ± 0.1	2.3 ± 0.4	3.0 ± 0.1	3.7 ± 0.1
CEM III/C	1.2 ± 0.1	2.8 ± 0.4	5.9 ± 0.6	7.1 ± 0.5
AAS-OH	1.3 ± 0.1	4.6 ± 0.1	8.2 ± 0.3	8.9 ± 0.2
AAS-SiO	0.2 ± 0.1	0.9 ± 0.1	8.9 ± 0.4	13.7 ± 0.6
AAS-CO	0.0	0.0	0.0	-

At the same time, OPC-stabilized soil samples showed a limited development in strength through time starting at 1.6 MPa, which was satisfactory regarding the initially stated requirements, and reaching a 60 days compressive strength that was barely double its early age value. This rather restricted evolution in time was noted as a common feature of OPC in presence of high water content [11]. In contrast, the slag-rich binder (CEM III/C) was able to develop the required minimal performance after 3 days of curing and compressive strengths twice those of OPC treatment alone after both 28 and 60 days. Sodium metasilicate activated GGBS displayed the most specific mechanical behavior. Samples developed low performances at early ages of curing (3 and 7 days), never achieving the required strength for trafficability of the subbase layer. After 28 days, and even more significantly after 60 days of curing, the unconfined compressive strengths of the AAS-SiO stabilized mud exceeded all other mix designs, reaching a final value about twice that of the more conventional CEM III/C mix design. Finally, the sodium carbonate activation of GGBS (AAS-CO) did not produce any mechanical performance at all for the first 28 days of curing. No measurements were performed at 60 days' curing for this mix. The development, or lack of development, of performance of alkali-activated GGBS stabilized mud is assessed further on in this work.

4.2. Isothermal calorimetry

Figure 2 displays the isothermal calorimetry results obtained for measurements performed during 7 days at 20 °C for the five different mix designs of stabilized mud.
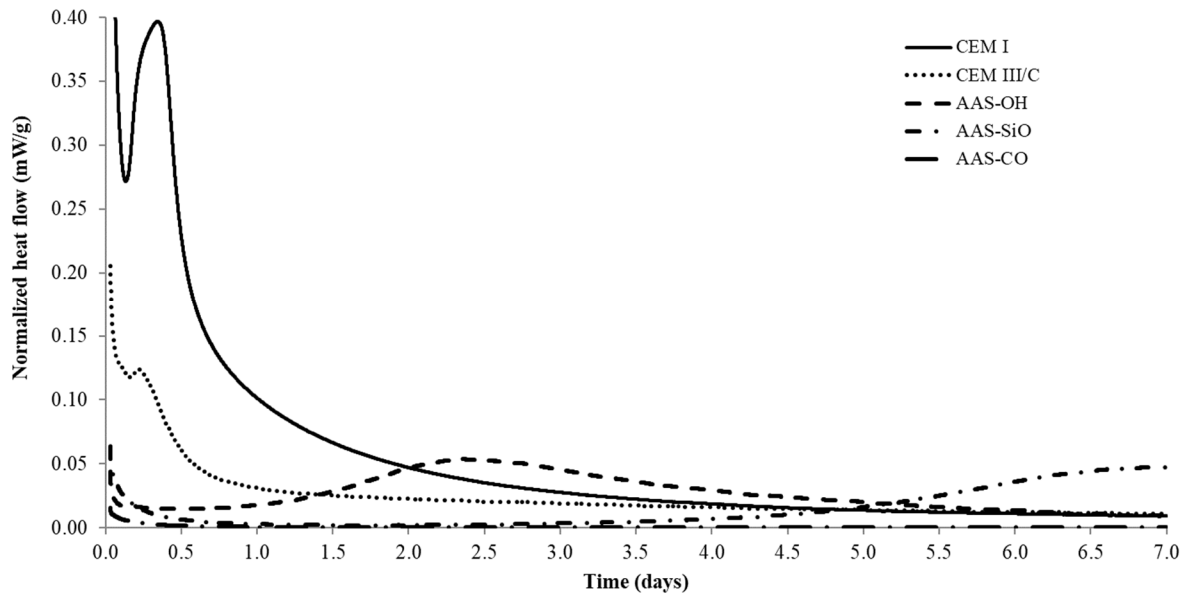
Figure 2 – Normalized heat flow for soil stabilized with each of the five binders.

In agreement with the absence of mechanical performance for the AAS-CO mix, isothermal calorimetry showed no heat flow during the entire period of measurement, hence a total heat flow equal to zero (Table 5). The other two alkali-activated mixes displayed significantly delayed heat release when compared to the conventional binders (CEM I and CEM III/C) and the time to reach peak (TTRP) remained below the usual 10 hours for these last two binders [29] (see Table 5). Sodium hydroxide activation TTRP was around 2.5 days and the sodium silicate activation peak was obtained at the very end of the measurement, i.e. after 7 days of hydration. In the case of sodium silicate activation, this delay corresponded to the lack of compressive strength after 3 and 7 days of curing (Table 4).

Table 5 – Time to reach peak and total heat flow for each of the five mix designs.

	TTRP (h)	Total Heat Flow (J/g)
CEM I	8.5	34.4
CEM III/C	5.5	14.9
AAS-OH	57.4	15.8
AAS-SiO	168	8.5
AAS-CO	-	~ 0

Total heat flow developed by pure Portland treated soil was more than two times the value measured when treatment was performed with the slag-rich binder (CEM III/C) or with the sodium hydroxide activated slag binder. As the reaction was expected to be incomplete for the sodium silicate activation at the end of the measurement, no comparison could be made.

4.3. In-situ pH

Figure 3 shows the in-situ pH value obtained on prismatic samples for three different soil-binder mixtures: when the treatment was performed with the slag-rich binder (CEM III/C) or with the NaOH activated slag binder or eventually with the Na_2SiO_3 activated slag. Measurements were stopped as soon as setting occurred, i.e. at the moment when the operator considered that the force

required to insert the pH probe would potentially damage it. Setting occurred roughly 5 hours after mixing in the case of the slag-rich binder treatment and about 48 hours after mixing for the AAS-SiO stabilization. In the case of sodium carbonate activated slag, measurements were stopped after 48 hours even though setting had not occurred. Raw soil displayed a slightly basic pH value of around 8.4.
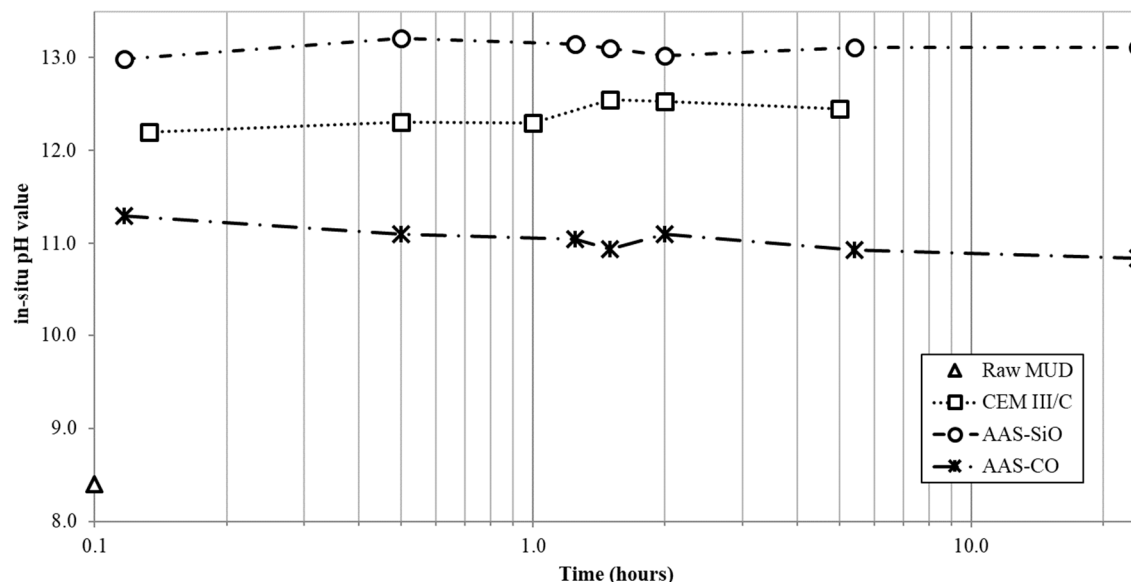

Figure 3 – In-situ pH values for the untreated soil, the CEM III/C stabilized soil, the sodium silicate activated slag stabilized soil and the sodium carbonate activated slag stabilized soil.

In the case of Na_2CO_3 activation, the pH value varied between 11.1 and 10.9 for the entire period of measurements. Such a value was considered to be insufficient to enable rapid dissolution of GGBS particles, which would have further on led to the development of hydrated phases and thus the accompanying mechanical performances at the required ages. In the case of sodium silicate activation, although pH values remained above 13 throughout the 48 hours timeframe between the end of the mixing protocol and the occurrence of setting, almost no compressive strength was measured at the 3 days curing time. At the same time, the CEM III/C based soil treatment developed an in-situ pH value around 12.3 to 12.5 for the five hours of open time offered by such a mix, which was consistent with its good reactivity.

4.4 Pore solution compositions

This part focuses on the properties and compositions of the pore solutions obtained at three different curing ages and for the four different mix designs of stabilized mud. Figure 4 summarizes the pH values obtained on the extracted pore solutions.
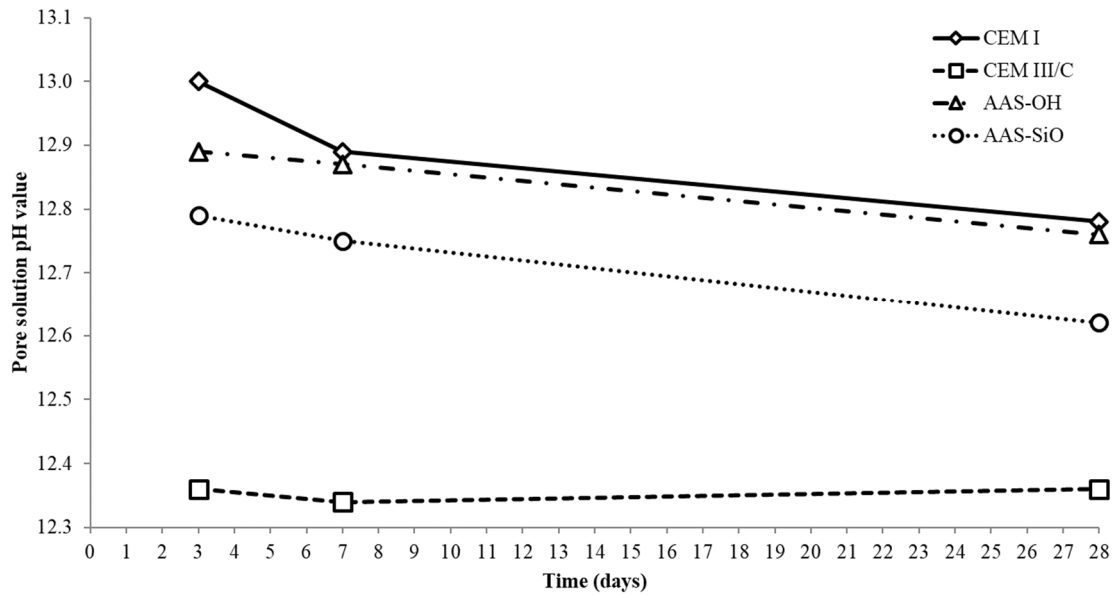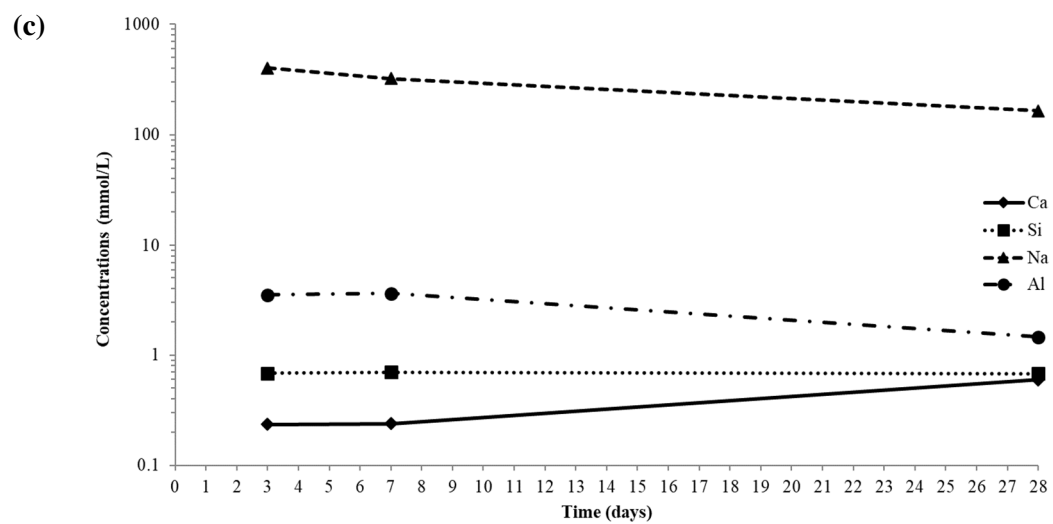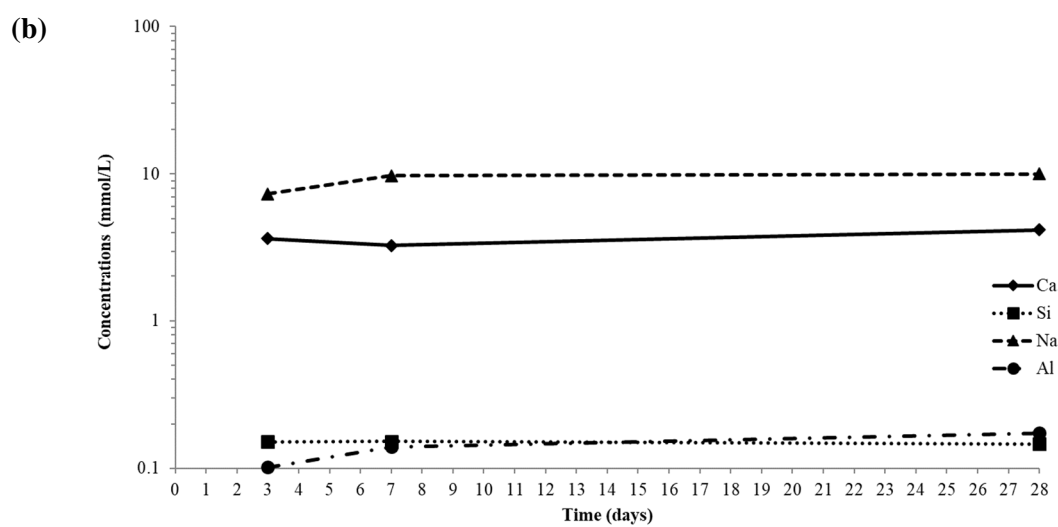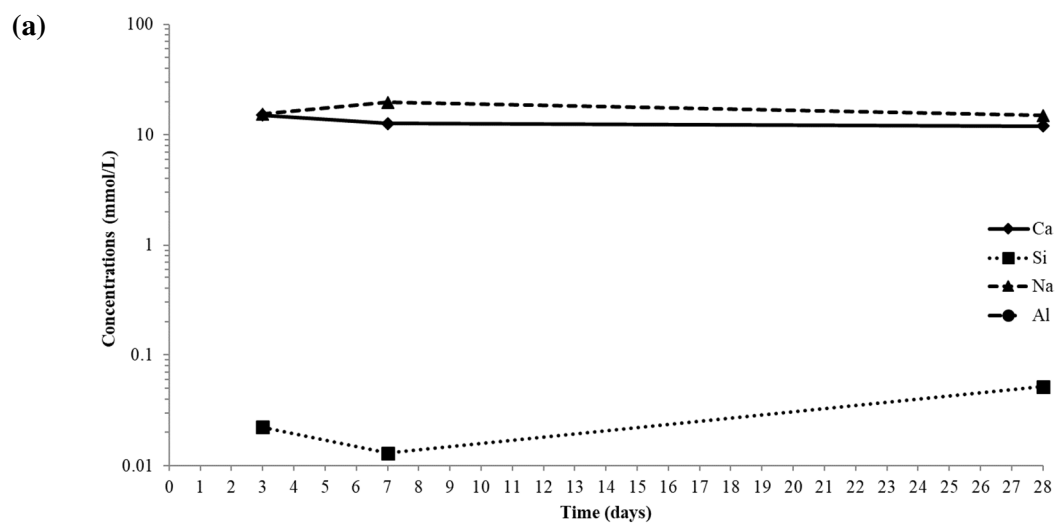
Figure 4 – pH evolution of extracted pore solutions with time for soil stabilized with four different binders.

The pH values measured directly after extraction showed a steady decrease with time for all mixes except for the slag-rich binder (CEM III/C), which displayed a relatively constant value around 12.35 for the 28 days timespan covered in this work.

Figure 5 gives the concentrations of the main constituents, i.e. calcium, silicon, aluminum and sodium, for the three curing durations and for the four types of binder-stabilized soil. In the case of pure OPC treatment (Fig. 5a), the pH decrease noted in Figure 4 was due to the slow, continuous consumption of the alkalis, sodium and essentially potassium (not measured here) initially contained in the OPC from the pore solution [36]. In the case of the CEM III/C samples (Fig. 5b), the constant concentrations of calcium and sodium corresponded to the steady pH value of the pore solution, showing a slower yet continuous hydration rate of GGBS in the soil environment. In agreement with [37], a constant pH of GGBS-rich pore solution binders was expected because of the glassy structure and therefore slower reactivity of this cementitious addition. Silicon concentrations for regular binders were relatively low because of its low solubility in this range of pH values (Figs. 5a and 5b). Due to the OPC chemical composition (Table 2), concentrations in aluminum were below the detection limit of the apparatus (not plotted in Fig. 5a).
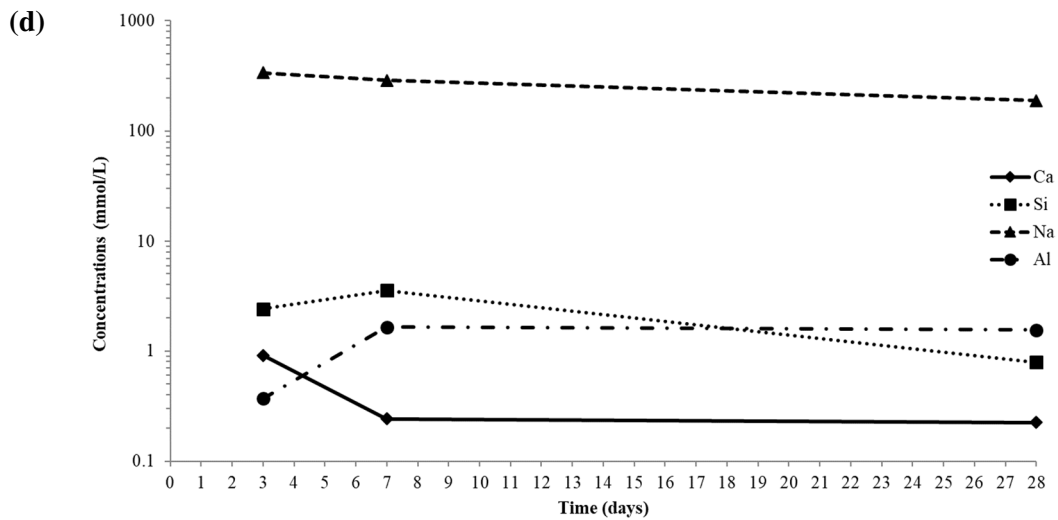
(a)

(b)

(c)

(d)

Figure 5 – Pore solution composition evolution through time for (a) CEM I stabilized soil, (b) GGBS-rich blended cement stabilized soil, (c) sodium hydroxide activated slag stabilized soil and (d) sodium metasilicate activated slag stabilized soil.

As shown in Figs. 5c and 5d, a similar process took place with the alkali-activated binders. The sodium concentration decrease was associated with its uptake by C-A-S-H hydrated phases. In the case of the AAS-SiO extracted solutions (Fig. 5d), the silicon concentrations were significantly higher than for other binders because of the activator contribution but also showed a decrease in time, again associated with C-A-S-H formation. In the work presented by Puertas et al. [38], pore solutions of alkali-activated GGBS were studied for the first seven days of hydration. Those solutions were extracted from paste samples that were prepared with a water to binder ratio of 0.5 and a total equivalent sodium oxide content of $Na_2O_{eq} = 4\%$. Activation with both sodium hydroxide and sodium silicate, presenting a molar ratio of $SiO_2/Na_2O = 1.5$, were evaluated. In our study, samples of stabilized mud with a water to binder ratio between 3.0 and 3.5 were prepared (Table 3), with a total equivalent alkali oxide content of $Na_2O_{eq} = 6\%$ and sodium metasilicate (molar ratio equal to 1.0). By applying suitable factors to the calculated species concentrations to take those differences into account, it was found that the evolution of sodium and silicon concentrations of both types of alkali-activated slag mixes (AAS-OH and AAS-SiO) agreed with the data presented in [38]. For AAS-SiO stabilized soil samples, the concentration profile through time for calcium was significantly higher after 3 days than the one reported in [38]. On the other hand, aluminum concentration for the same mix design was reported to be lower than the same original dataset. It is noteworthy that pore solutions from sodium metasilicate stabilized soils showed a gradation in color through time with a thick dark solution after 3 days of curing, an orange solution after 7 days and light yellow one after 28 days.

4.5. Thermogravimetric analysis

Figure 6 gives the first derivative of thermogravimetric acquisitions (DTG) for the paste samples of sodium hydroxide and sodium silicate activated slag at 3 and 28 days of curing. For all samples, four main peaks are identified, following literature referencing in [29]. Between 100 and 150 °C, the main peak is associated with dehydration of C-A-S-H, which was the main hydrated phase of such systems [39-41]. Peaks at 200-250 °C and 350-400 °C were directly related to the Mg-Al layered double hydroxides, often identified in alkali-activated slags as hydrotalcite destructuring. The last main peak, particularly visible for sodium metasilicate activated samples and situated between 800 and 850 °C, was associated with decarbonation. Carbonated phases were expected to be formed due to waiting time before testing and insufficiently well sealed storage conditions.
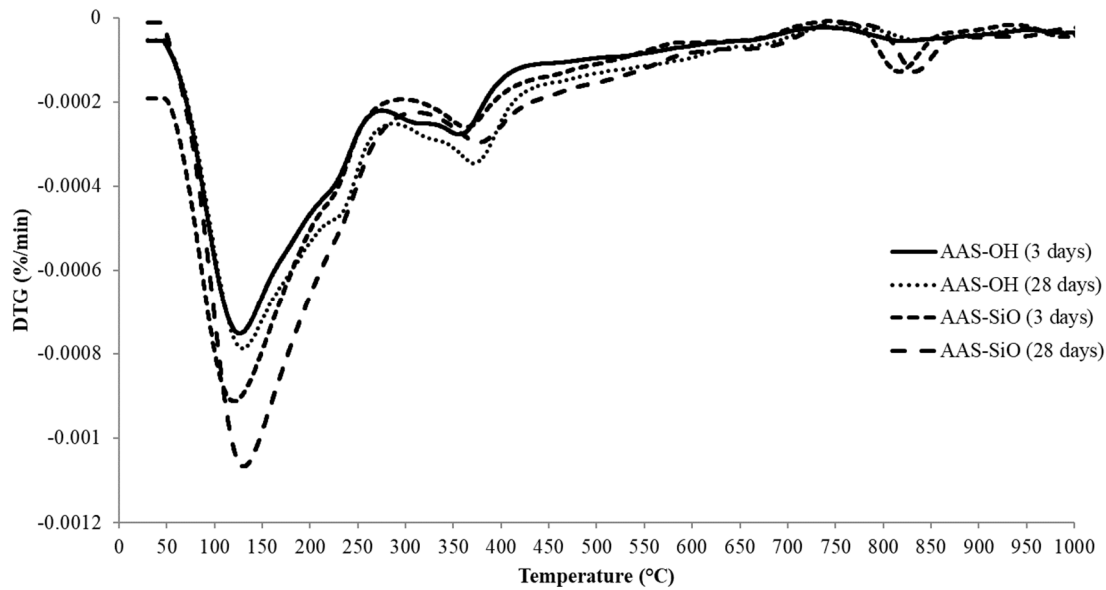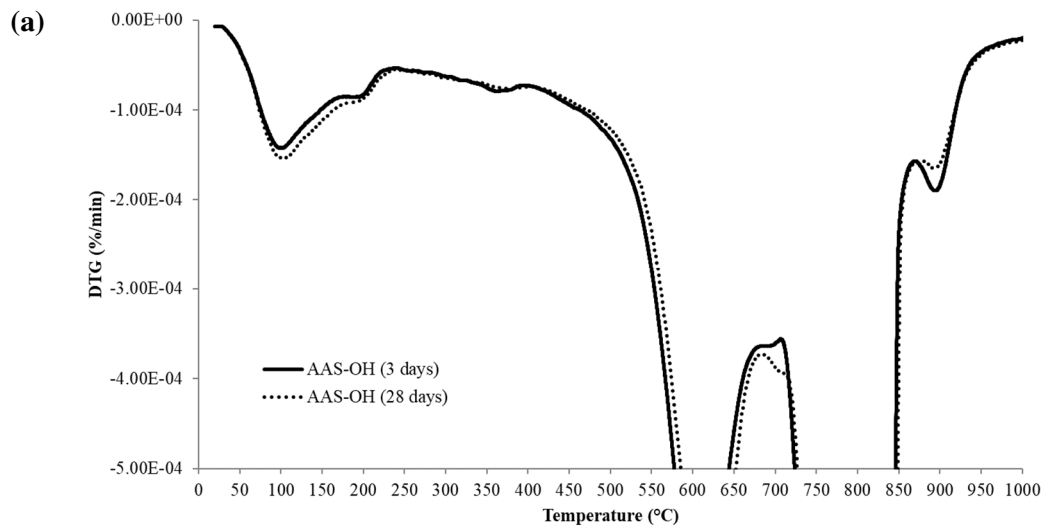
Figure 6 – First derivative curves of thermogravimetric analysis of sodium hydroxide and sodium metasilicate activated GGBS paste samples after 3 and 28 days of sealed curing.

In the case of sodium metasilicate activation, the peak associated with C-A-S-H appeared with higher amplitude at the same curing ages relative to sodium hydroxide activation, which was related to the formation of a higher amount of this hydrated phase, mostly due to the supply of fast soluble silicon ions in solution from the alkaline activator.

Stabilized soil samples with same the mix types were also analyzed, at the same curing times, following the same preparation (solvent exchange method) and testing (5 °C/min) protocols. As confirmation of the XRD measurement (Fig. 1), main DTG peaks at 600 °C and 800 °C, partially omitted from Figs. 7a and 7b, were associated with decarbonation of dolomite (both peaks) and calcite (second peak).
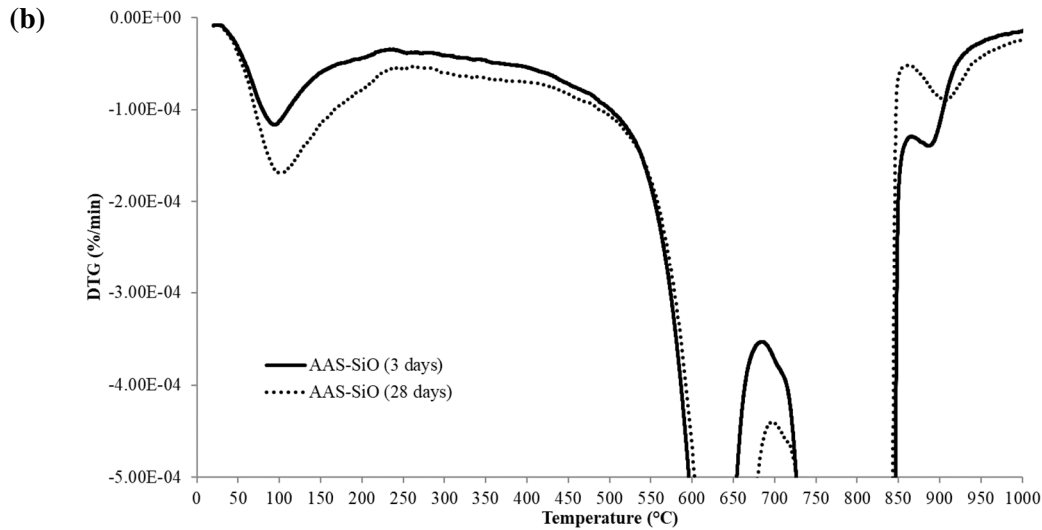
Figure 7 - First derivative curves of thermogravimetric analysis of stabilized soil samples after 3 and 28 days when using (a) sodium hydroxide activated slag and (b) sodium metasilicate activated slag.

As shown in Fig. 7a, sodium hydroxide activated GGBS stabilized soil led to the formation of the two main hydrated phases identified in the pure pastes, i.e. C-A-S-H (100-150 °C) and hydrotalcite (both 200-250 °C and 350-400 °C) at 3 and 28 days. Hydrated phase amounts evolved slightly between the two durations of curing tested here (3 and 28 days), mostly with an increase in the C-A-S-H related peak. In the case of AAS-SiO samples (Fig. 7b), only C-A-S-H was clearly identified from the DTG after 3 and 28 days of curing. In the latter case, peak intensity evolution was significantly more marked than for AAS-OH samples, moving from the lowest intensity at 3 days, even lower than AAS-OH samples, to the highest noted at 28 days. The absence of peaks related to Mg-Al layered double hydroxides, for this particular mix design, could be attributed to the consumption of aluminum atoms by either C-A-S-H formation or complexation by organic matter, as often pointed out in the literature [42].

The small DTG peak intensity of AAS-SiO at early age, followed by a sudden increase in C-A-S-H peak after 28 days' curing, was in good correlation with the unconfined compressive strength developments noted in Table 4. As for AAS-OH, well defined peaks for the two main hydrated phases at both early and long curing ages confirmed the good reactivity of this type of binder, and hence the accompanying satisfactory mechanical performances at all ages when used in soil stabilization.

In all cases presented in Fig. 7, the peak appearing between 900 and 950 °C could not be associated with mineral phases, either originating in the raw soil or from hydrated alkali-activated binders. The scientific literature reports [43] potential destructuring of organic matter, either in its raw molecular form or when complexing metallic atoms, in this temperature range.

5. Organic matter characterization

The following paragraphs mainly deal with the organic matter naturally present in the soil used for this study. According to the protocols described in paragraph 3, organic matter was first extracted from the soil with solutions containing the different alkaline activators. Such solutions were then either directly analyzed with the Folin-Lowry method to calculate the concentrations of humic substances or passed through a multi-step process so that the precipitated substances could be analyzed with infrared spectroscopy and by scanning electron microscopy.

5.1. Organic matter extraction

Organic matter extractions were performed following the protocol steps described in 3.7 using the three different alkaline sources of interest. As described in standard [30], filtered supernatant solutions were compared to a standard color solution, a mixture of $FeCl_3$, $CoCl_2$ and HCl (also called Gardner Color Standard Number 11). With the standardized protocol, it was considered that the test for humic acid presence was positive if the supernatant solution was darker than the Gardner standard and negative if not.

Table 6 – Supernatant solution pictures, alkaline composition and pH measured after extraction.

Alkali source	*NaOH*	*Na₂CO₃*	*Na₂SiO₃*
Supernatant solution			
%Alkali (mass)	3.0%	4.0%	4.6%
pH (supernatant solution)	12.8	11.1	12.8

As shown in Table 6, supernatant solutions displayed a significantly different color depending on the alkali source, even though the concentrations of the initial solutions were prepared in order to maintain the Na_2O_{eq} constant. The NaOH-extracted solution was considered negative regarding the Gardner Color Standard (brighter), the Na_2SiO_3-extracted solution positive and the Na_2CO_3-extracted solution was visually at our decisional limit. Table 6 also indicates the pH values of the supernatant solutions. It was noted that no obvious relation existed between the pH value of a solution and its color.

5.2. FTIR

After applying the precipitation and drying steps described in 3.7 for both humic and fulvic acids extracted with the three different alkaline activators, Fourier Transform Infrared Spectroscopy (FTIR) was performed. As mentioned in 3.7, no NaOH-extracted humic acid was retrieved, and therefore analyzed, in this work. Due to the complexity and variety of molecular structures when considering humic acid and fulvic acid [21], identifying each and every vibration peak out of a given spectrum appeared to be difficult. Nevertheless, based on the thorough listing provided in [44,45], main organic chemical functional groups were identified from the measurements. Figure 8 gathers together the humic acid spectra for precipitated sodium metasilicate and carbonate extractions. Figure 9 shows the fulvic acid spectra for precipitated sodium metasilicate, carbonate and hydroxide extractions. The main peaks identified for both organic acid groups are listed below.
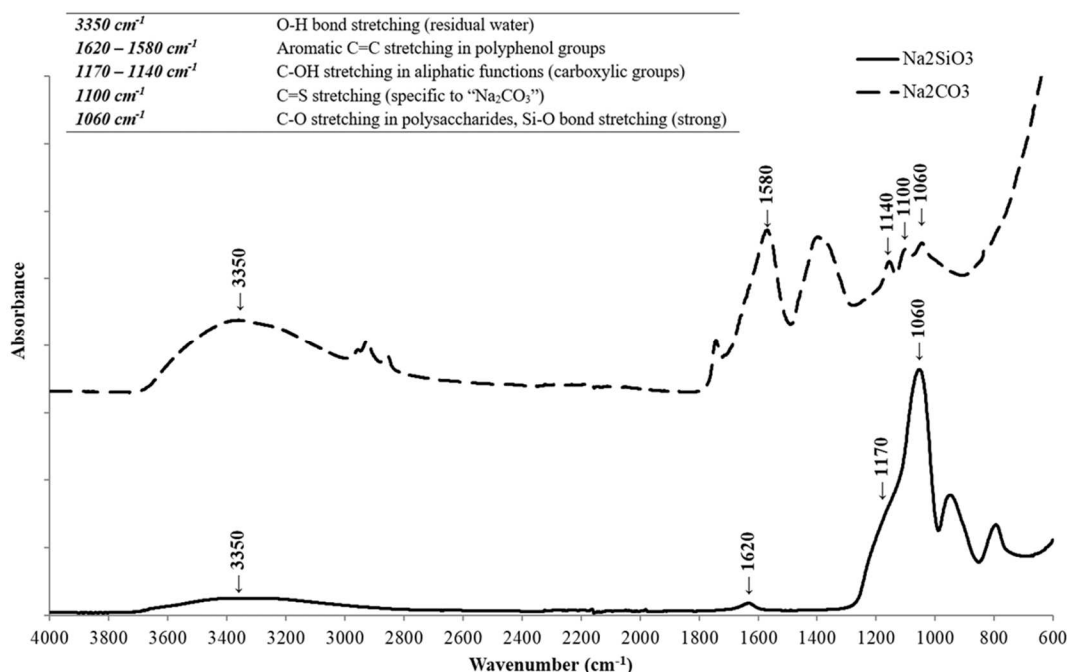
3350 cm⁻¹	O-H bond stretching (residual water)
1620 – 1580 cm⁻¹	Aromatic C=C stretching in polyphenol groups
1170 – 1140 cm⁻¹	C-OH stretching in aliphatic functions (carboxylic groups)
1100 cm⁻¹	C=S stretching (specific to "Na₂CO₃")
1060 cm⁻¹	C-O stretching in polysaccharides, Si-O bond stretching (strong)

Figure 8 – FTIR spectra of precipitated humic acids obtained from Na_2SiO_3 and Na_2CO_3 solutions and associated atomic bond vibrations.

For both activators, the precipitated humic acids displayed several similar functional groups (Fig. 8). The vibrations occurring around 3350 cm⁻¹, 1620-1580 cm⁻¹ and 1170-1140 cm⁻¹ were respectively associated with O-H stretching (in residual water for example), aromatic C=C stretching in polyphenol groups and C-OH stretching in aliphatic functions (carboxylic group). The two species were differentiated mostly in the wavenumber range of 1100-1000 cm⁻¹. For sodium carbonate extraction, two peaks were distinguished: the one at approximately 1060 cm⁻¹ was associated with C-O stretching in polysaccharides, according to [44], while the sharp peak at 1100 cm⁻¹ was potentially associated with the double bond between a carbon atom and a sulfur atom, as described by [46]. In the case of sodium metasilicate extraction, the peak at 1060 cm⁻¹ was a major vibrational response of the entire spectrum. Given its significant breadth and amplitude, and the type of alkaline activator initially used for the extraction, it was assumed that this peak corresponded to vibration of Si-O bonds.
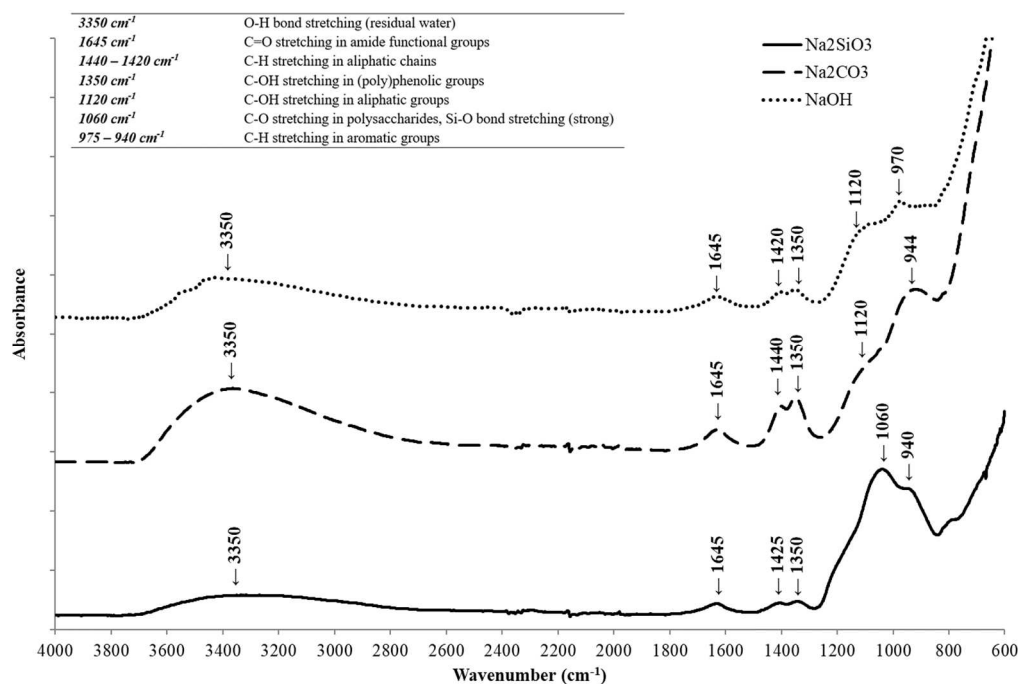
Figure 9 – FTIR spectra of precipitated fulvic acids obtained from the three different alkaline activators and associated atomic bond vibrations.

In the case of fulvic acids, five peaks were found for all three types of extraction (Fig. 9):

- again, around 3350 cm^{-1} for the O-H stretching,
- at 1645 cm^{-1} for C=O stretching in amide functional groups,
- between 1440 and 1420 cm^{-1} for C-H stretching in aliphatic chains,
- at 1350 cm^{-1} for C-OH stretching in (poly)phenolic groups,
- between 975 and 940 cm^{-1} for C-H stretching in aromatic groups.

For both sodium hydroxide and sodium carbonate extractions, a peak was also partly visible in the spectra around 1120 cm^{-1} and, as for humic acids, was potentially associated with C-OH stretching in aliphatic functions. Finally, in the case of Na$_2$SiO$_3$ extracted solution, the major peak identified in the fulvic acid spectrum occurred around 1060 cm^{-1} and, considering the type of alkaline activators and possible atom bond vibrations considered in [45], was eventually associated with Si-O bonds. With regard to the FTIR spectra of humic and fulvic acids extracted with sodium metasilicate, it appeared that, after the precipitation and drying steps defined in 3.7, large quantities of silicon were integrated into the molecular structure of these organic acids.

5.3. Folin-Lowry method

Humic acid and animal protein concentrations in each of the solutions extracted according to the protocol described in 3.7, and displayed in 5.1, were obtained by applying the Folin-Lowry method and calculated with the help of equations (3) and (4). In the particular case of proteins, related calculated absorbance at 750 nm for all three activator solutions was either lower than or of the same amplitude as the absorbance of blank solutions, with reagents A and B. Protein concentrations in extracted solutions were then considered to be equal to zero, which was expected for soil excavated in a tunnel boring process (several tens of meters below the surface). At the same time, humic acid absorbances showed large variations from one extracted solution to another, as could have been expected from the color gradation observed in Table 6.
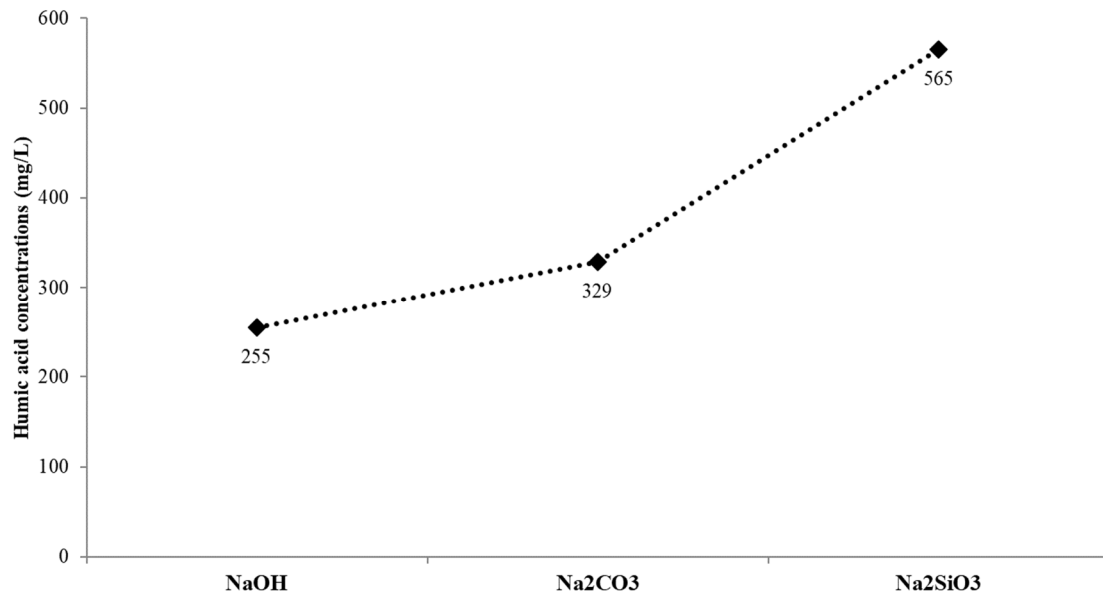
Figure 10 – Humic acid concentrations in extracted solutions depending on the alkaline activator.

As summarized in Fig. 10, humic acid concentrations increased with both the molecular weight of the alkaline activator and the blackness of the extracted solution (Table 6). Though they displayed identical pH values, sodium silicate extraction led to a concentration in humic acids more than twice as high as the one obtained with NaOH. However, no direct relation could be established between the calculated concentrations and the pH value of the extracted solutions or the molecular weight of the alkaline activator. As noted in [47], humic acids are strong complexing agents of soluble calcium. In our case, this increase in dissolved humic acid concentration with the change of alkaline activator was directly associated with the delay in compressive strength development observed for sodium metasilicate activated slag (Table 4) compared to sodium hydroxide activated GGBS stabilized soil. As for Na_2CO_3 activated slag stabilized samples, the absence of solidification even after 28 days of curing was associated with both the low in-situ pH value (Fig. 3) and the intermediate amount of humic acid that was potentially extracted with such an alkaline activator.

5.4. SEM-EDS of organic acids

Scanning Electron Microscopic images of organic acids were always obtained coupled with elemental chemical composition through EDS measurement. Exclusively humic and fulvic acids extracted with sodium metasilicate, and precipitated according to the protocol defined in 3.7, were observed by these means. Figure 11 summarizes the main observations made at the micrometric scale of the materials. Figure 11a gives a global view of precipitated humic acid particles. Figure 11b focuses on a single particle of the humic acid. Figure 11c also gives a global view of precipitated fulvic acid particles. Fig. 11d focuses on a single particle of fulvic acid.

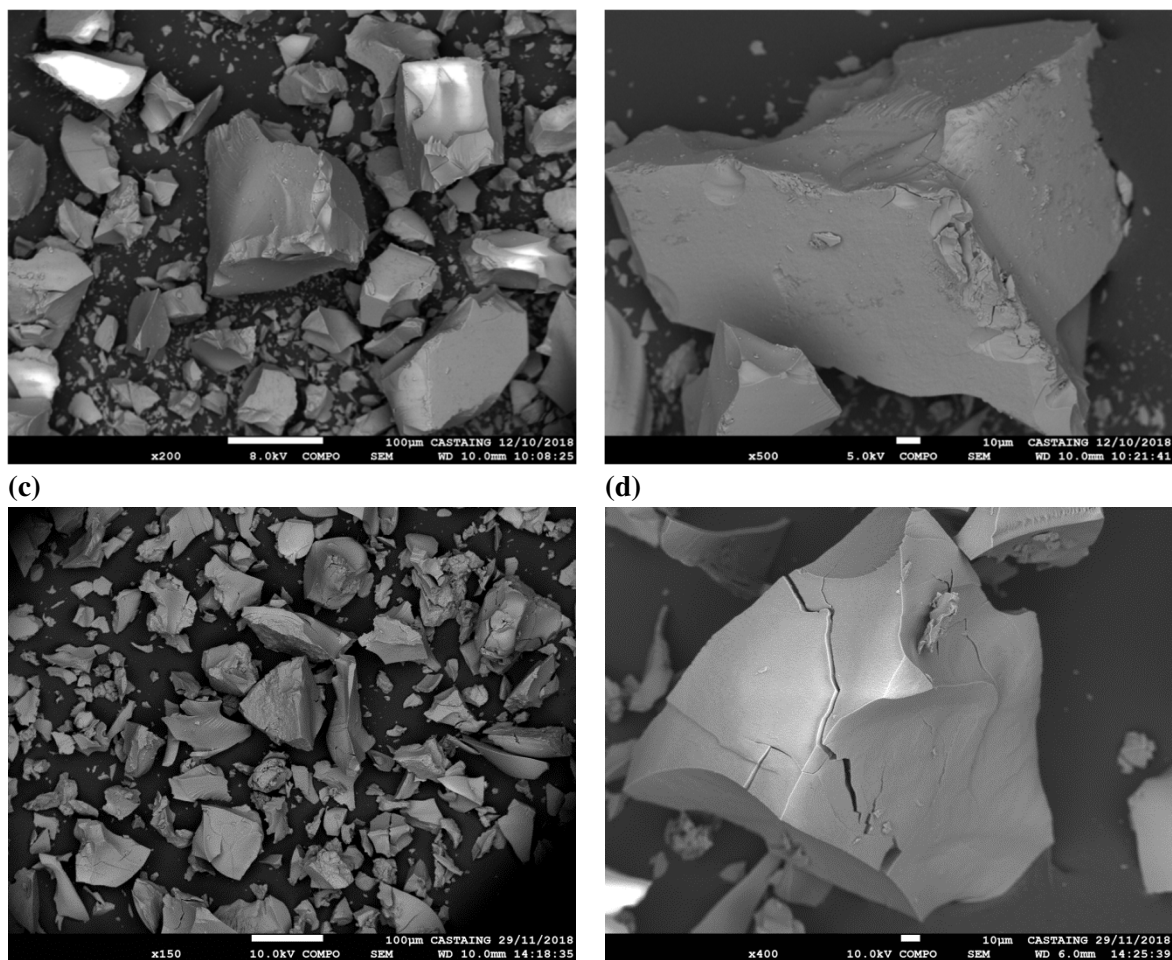**(a)**   **(b)**

Figure 11 – SEM images of precipitated organic matter: (a) global view of precipitated humic acid particles from Na_2SiO_3 solution (b) focus on one particle of humic acid of the same type (c) global view of precipitated fulvic acid particles from Na_2SiO_3 solution (d) focus on one particle of fulvic acid of the same type.

From the SEM observations, it was noted that all particles had a glass like surface aspect and displayed very good visual homogeneity after the precipitation-drying process. Up to 60 different areas per organic acid type were analyzed with the EDS to obtain an estimated elemental composition. The results are summarized in Table 7 in the form of average value plus or minus standard deviation.

Table 7 – EDS atomic compositions of sodium-metasilicate-precipitated humic and fulvic acids.

Chemical Element	Oxygen	Silicon	Aluminum	Chlorine	Sulfur	Carbon
Humic acid (Na_2SiO_3)	54.5 ± 2.1	37.8 ± 3.1	-	-	-	7.7 ± 2.6
Fulvic Acid (Na_2SiO_3)	58.1 ± 3.1	18.3 ± 3.2	11.9 ± 1.3	2.0 ± 0.3	0.3 ± 0.1	9.4 ± 2.6

For the two types of samples presented in Table 7, even though the powders analyzed were precipitated organic acids, the amount of carbon measured at the EDS was very low, around 8% and 9% for the sodium metasilicate extracted humic and fulvic acids respectively. Also, it appeared that both these materials had a high silicon content (around 38% for the humic acid and 18% for the fulvic acid). These observations confirmed the previous results obtained with infrared spectroscopy (Figs. 8 and 9) where vibration wavenumbers associated with Si-O bonds were observed and, in the case of humic acid, formed the major peak of the spectrum. Due to the presence of polyphenol groups in their

structure [48-51], these organic acids demonstrated a great complexing capacity towards silicon atoms dissolved from the alkaline activator [52]. This high silicon complexing ability was considered to be an additional argument, with the calcium and aluminum complexations noted before, for the delayed development of mechanical performances of sodium metasilicate activated slag stabilized soil samples, through a delayed formation of the main hydrated phases.

In the case of the fulvic acid, significant amounts of aluminum and chlorine were also measured. Their presence was assumed to originate exclusively in the precipitation protocol involving AlCl$_3$, as described in 3.7. Minor traces of sulfur were also detected in this category of organic acid. As noted in [53,54], sulfur atoms can be closely integrated in the molecular structure of both humic and fulvic acids.

6. Discussion

From the results presented in the previous paragraphs and the initial discussions that emerged from them, we attempted to draw a reactivity scheme for the different types of binders used in this work and especially for alkali-activated slag when employed in the framework of soil stabilization/solidification. As seen before, the reactivity of alkali-activated slag in this environment was found to be strongly dependent on the alkaline activator used. At the same time, organic matter, naturally occurring in soils, also showed significant interactions with dissolved ions from the different activators.

6.1. CEM I and CEM III/C

Treatment performed with pure OPC (CEM I) led to sufficient mechanical performances after 3 days of curing. Its development in the longer term was the least efficient among all five binders tested in this study. This lack of compressive strength development was essentially due to the high water content of the stabilized mud samples, which were prepared with a water to binder ratio of 3.5, the moderate amount free alkalis, and the high solubility of calcium from cement particles, which could lead to complexation with humic substances.

The GGBS-rich binder (CEM III/C) demonstrated very good reactivity when used in soil stabilization/solidification. It outperformed pure OPC treatment after only 7 days, whereas this type of binder usually takes several weeks or months to give comparable results when used in regular concrete applications. The slower hydraulic reactivity of the GGBS, characterized by a lower hydration pH, between 12 and 12.5, enabled the continuous development of a denser microstructure. The limited amount of free alkalis available in the constituents restricted the impact of organic matter on the hydration of the binder. After consideration of the mixture proportions, clinker activation of GGBS was noted as the most suitable solution for soil solidification in subbase layer development, especially in the context of upcycling tunnel boring muds with high water content.

6.2. NaOH activated GGBS

The NaOH activation showed the most promising results in terms of mechanical performance development through time. Humic acid extracted with this alkaline molecule had the lowest concentration of all three activators. FTIR spectra of the precipitated fulvic acid showed no peculiar peak and therefore we assumed no significant molecule modification. When this type of binder was used for soil solidification, both GGBS particle dissolution and clay-humus breakdown were initiated with the addition of sodium hydroxide. Competition took place between precipitation of hydrated phases, C-A-S-H and hydrotalcite, as shown by TGA measurement, and complexation by humic

substances of dissolved calcium, aluminum and silicon from GGBS. Due to the relatively small amount of humic acid extracted and the slower dissolution rate of slag particles, hydration was slightly delayed as identified by isothermal calorimetry but not enough to affect mechanical performances development within the limited timeframe chosen (3 days).

6.3. Na₂SiO₃ activated GGBS

The sodium metasilicate activation showed a two-sided response, with no or very low unconfined compressive strengths for the first seven days of curing followed by a sudden continuous increase after 28 and 60 days. The humic substances extracted showed drastic modifications compared to hydroxide-based solutions. Humic acid concentration in solution was the highest, at more than double that obtained with sodium hydroxide. Both humic and fulvic acid showed an additional ability for silicon complexation. As described before, insertion of alkaline activator in GGBS-soil mixture led to competitive processes: dissolution of the glassy structure of slag particles and release of humic substances in solution. Because of both the very large amount of humic substances extracted and their ability to integrate soluble silicon brought by the activator in combination with dissolved calcium [55] and aluminum from slag [56], the formation of hydrated phases was strongly delayed, up to 7 days according to isothermal calorimetry measurements. This complexing ability of humic substances was also confirmed in pore solution extractions from AAS-SiO samples with an excess of calcium after three days. This excess came from the acidification of the pore solution for conservation purposes, which led to the rupture of the calcium – carboxylic function bond. As noted with the in-situ pH measurements up to 48 hours and pore solution pH values up to 28 days, AAS-SiO constantly developed a highly basic environment, which was maintained throughout curing. As noted in [57], such an environment could have promoted degradation of humic substances through an autoxidation process, breaking down high molecular weight humic acid structures into smaller molecules. As also noted from color changes in pore solutions extracted from this type of samples and the sudden evolution of mechanical performances in time, the autoxidation process was expected to destabilize the complexing ability of humic substances in solution, thus increasing the availability of species such as silicon and calcium for the precipitation of hydrated phases.

6.4. Na₂CO₃ activated GGBS

Finally, the activation with sodium carbonate (AAS-CO samples) was the least suitable solution for subbase layer construction. For the 28 days curing period evaluated in this work, it never developed any mechanical performances. The amount of humic acid extracted was intermediate between those obtained with sodium hydroxide and sodium silicate, though the pH value of the corresponding solution was significantly lower than for the other two alkaline activators: 11.1 instead of 12.8. In-situ pH measurements gave values that were expected to be too low for rapid enough reactivity within the required curing times. The hydration of sodium carbonate activated slag is described in [58] as a two stages process. First, the rise in pH up to 11-11.5, associated with the dissolution of sodium carbonate, leads to a slow dissolution of GGBS particles. Freed calcium ions form amorphous $CaCO_3$ by combining with the carbonate initially inserted with the activator. At more advanced times, when enough carbonate anions are combined with calcium, the pore solution pH rises through the production of NaOH in situ, which accelerates the hydration process. This two steps process generally develops strong mechanical performance after three days. In the case of AAS-CO samples, hydrated phase formations then had to face two competitive chemical processes: calcium consumption for amorphous calcium carbonate production and calcium capture by carboxylic groups of humic acid in basic pH environment. Though degradation of the humic substances in an alkaline environment [57] and therefore calcium release into the solution was expected to occur, as for sodium

metasilicate activation, it was not expected to take place within an acceptable timeframe for the targeted application. Providing an initial amount of soluble calcium to the system, in the form of quicklime for example, could be a solution to counteract the two deleterious processes identified and accelerate the hydration process.

7. Conclusions

This study focused on the development of a subbase layer for road construction from solidified tunnel boring muds with alkali-activated slag. The efficiency of three different alkaline activators on slag solidification of one calcareous type of soil was evaluated. In addition to previous findings presented in the scientific literature, it was noted that humic substances, including both humic and fulvic acids, were strong complexing agents, not only of dissolved calcium and aluminum but also of silicon in solution. At the same time, alkaline extraction of humic substances from the soil proved to be source dependent. Measured humic acid concentration increased by more than a factor of two with the increase in molecular mass of the alkaline activator. As a result, sodium hydroxide activated slag, even though it displayed a slightly delayed reactivity as identified in isothermal calorimetry measurements proved to be a suitable solution for the solidification of tunnel boring muds within the time frame and mechanical performance requirements set for the chosen application. On the other hand, even though it usually shows the most promising performances in general concrete applications, sodium metasilicate activation did not meet the early age compressive strength requirement. Combination of high humic acid concentration and complexing of dissolved calcium, silicon and aluminum, all essential elements in the formation of hydrated phases, turned sodium silicate activated slag into an unsuitable solution for rapid soil solidification and hence subbase layer development. In the case of sodium carbonate activation, the intermediate humic acid concentration level coupled with lower pH environment made the use of plain Na_2CO_3 activated GGBS improper for soil solidification within the studied time frame (up to 28 days). Eventually, the highly corrosive character and relatively high cost of NaOH and Na_2SiO_3 mean that alkali-activated binders are unlikely to be widely used on working sites. This seems even more unlikely when we consider that a conventional binder containing up to 90 % GGBS and 10% OPC was found to be a suitable solution, which also outperformed plain OPC treatment, for the solidification of tunnel boring muds for subbase layer realization.

References

[1] Trincal, V., Thiéry, V., Mamindy-Pajany, Y., & Hillier, S. (2018). Use of hydraulic binders for reducing sulphate leaching: application to gypsiferous soil sampled in Ile-de-France region (France). *Environmental Science and Pollution Research*, *25*(23), 22977-22997.

[2] Kuttah, D., & Sato, K. (2015). Review on the effect of gypsum content on soil behavior. *Transportation Geotechnics*, *4*, 28-37.

[3] Dubois, V., Abriak, N. E., Zentar, R., & Ballivy, G. (2009). The use of marine sediments as a pavement base material. *Waste Management*, *29*(2), 774-782.

[4] Saussaye, L., Van Veen, E., Rollinson, G., Boutouil, M., Andersen, J., & Coggan, J. (2017). Geotechnical and mineralogical characterisations of marine-dredged sediments before and after stabilisation to optimise their use as a road material. *Environmental technology*, *38*(23), 3034-3046.

[5] Behnood, A. (2018). Soil and clay stabilization with calcium-and non-calcium-based additives: A state-of-the-art review of challenges, approaches and techniques. *Transportation Geotechnics*, *17*, 14-32.

[6] Khadka, S. D., Jayawickrama, P. W., Senadheera, S., & Segvic, B. (2020). Stabilization of highly expansive soils containing sulfate using metakaolin and fly ash based geopolymer modified with lime and gypsum. *Transportation Geotechnics*, *23*, 100327.

[7] Coudert, E., Paris, M., Deneele, D., Russo, G., & Tarantino, A. (2019). Use of alkali activated high-calcium fly ash binder for kaolin clay soil stabilisation: Physicochemical evolution. *Construction and Building Materials*, *201*, 539-552.

[8] Ghadir, P., & Ranjbar, N. (2018). Clayey soil stabilization using geopolymer and Portland cement. *Construction and Building Materials*, *188*, 361-371.

[9] Sargent, P., Hughes, P. N., Rouainia, M., & White, M. L. (2013). The use of alkali activated waste binders in enhancing the mechanical properties and durability of soft alluvial soils. *Engineering geology*, *152*(1), 96-108.

[10] Abdeldjouad, L., Asadi, A., Nahazanan, H., Huat, B. B., Dheyab, W., & Elkhebu, A. G. (2019). Effect of Clay Content on Soil Stabilization with Alkaline Activation. *International Journal of Geosynthetics and Ground Engineering*, *5*(1), 4.

[11] Cristelo, N., Glendinning, S., Fernandes, L., & Pinto, A. T. (2013). Effects of alkaline-activated fly ash and Portland cement on soft soil stabilisation. *Acta Geotechnica*, *8*(4), 395-405.

[12] Cristelo, N., Glendinning, S., & Teixeira Pinto, A. (2011). Deep soft soil improvement by alkaline activation. *Proceedings of the Institution of Civil Engineers-Ground Improvement*, *164*(2), 73-82.

[13] Teing, T. T., Huat, B. B., Shukla, S. K., Anggraini, V., & Nahazanan, H. (2019). Effects of Alkali-Activated Waste Binder in Soil Stabilization. *International Journal*, *17*(59), 82-89.

[14] Cristelo, N., Glendinning, S., Miranda, T., Oliveira, D., & Silva, R. (2012). Soil stabilisation using alkaline activation of fly ash for self compacting rammed earth construction. *Construction and building materials*, *36*, 727-735.

[15] Alsafi, S., Farzadnia, N., Asadi, A., & Huat, B. K. (2017). Collapsibility potential of gypseous soil stabilized with fly ash geopolymer; characterization and assessment. *Construction and Building Materials*, *137*, 390-409.

[16] Feng, Y. S., Du, Y. J., Reddy, K. R., & Xia, W. Y. (2018). Performance of two novel binders to stabilize field soil with zinc and chloride: Mechanical properties, leachability and mechanisms assessment. *Construction and Building Materials*, *189*, 1191-1199.

[17] Kutuniva, J., Mäkinen, J., Kauppila, T., Karppinen, A., Hellsten, S., Luukkonen, T., & Lassi, U. (2019). Geopolymers as active capping materials for in situ remediation of metal (loid)-contaminated lake sediments. *Journal of Environmental Chemical Engineering*, *7*(1), 102852.

[18] Zhang, M., Zhao, M., Zhang, G., Nowak, P., Coen, A., & Tao, M. (2015). Calcium-free geopolymer as a stabilizer for sulfate-rich soils. *Applied Clay Science*, *108*, 199-207.

[19] Rios, S., Ramos, C., da Fonseca, A. V., Cruz, N., & Rodrigues, C. (2016). Colombian soil stabilized with geopolymers for low cost roads. *Procedia engineering*, *143*, 1392-1400.

[20] Phummiphan, I., Horpibulsuk, S., Rachan, R., Arulrajah, A., Shen, S. L., & Chindaprasirt, P. (2018). High calcium fly ash geopolymer stabilized lateritic soil and granulated blast furnace slag blends as a pavement base material. *Journal of hazardous materials*, *341*, 257-267.

[21] Vieyra, F. E. M., Palazzi, V. I., de Pinto, M. I. S., & Borsarelli, C. D. (2009). Combined UV–Vis absorbance and fluorescence properties of extracted humic substances-like for characterization of composting evolution of domestic solid wastes. *Geoderma*, *151*(3-4), 61-67.

[22] Lehmann, J., & Kleber, M. (2015). The contentious nature of soil organic matter. *Nature*, *528*(7580), 60.

[23] Kleber, M., & Lehmann, J. (2019). Humic substances extracted by alkali are invalid proxies for the dynamics and functions of organic matter in terrestrial and aquatic ecosystems. *Journal of Environmental Quality*, *48*(2), 207-216.

[24] AFNOR, S. (1993). Sols: reconnaissance et essais–Détermination des limites d'Atterberg–Limite de liquidité à la coupelle–Limite de plasticité au rouleau.

[25] AFNOR, N. 94-068 (1998). *Sols: reconnaissance et essais, "Mesure de la capacité d'adsorption de bleu de méthylène d'un sol ou d'un matériau rocheux-Détermination de la valeur de bleu de méthylène d'un sol ou d'un matériau rocheux par l'essai à la tache".*

[26] XP P 94-047. (1998). Soils: Investigation and testing–determination of the organic matter content–ignition method.

[27] AFNOR, N. N. (2001). EN 197-1-Ciment-Partie 1: composition, spécifications et critères de conformité des ciments courants.

[28] Cyr, M., Rivard, P., Labrecque, F., & Daidie, A. (2008). HighPressure Device for Fluid Extraction from Porous Materials: Application to CementBased Materials. *Journal of the American Ceramic Society*, *91*(8), 2653-2658.

[29] Scrivener, K., Snellings, R., & Lothenbach, B. (Eds.). (2018). *A practical guide to microstructural analysis of cementitious materials*. Crc Press.

[30] AFNOR, N. N. (2014) EN 1744-1, Essais visant à déterminer les propriétés chimiques des granulats - Partie 1 : analyse chimique.

[31] Hiradate, S., Yonezawa, T., & Takesako, H. (2006). Isolation and purification of hydrophilic fulvic acids by precipitation. *Geoderma*, *132*(1-2), 196-205.

[32] Lowry, O. H., Rosebrough, N. J., Farr, A. L., & Randall, R. J. (1951). Protein measurement with the Folin phenol reagent. *Journal of biological chemistry*, *193*, 265-275.

[33] Frølund, B., Palmgren, R., Keiding, K., & Nielsen, P. H. (1996). Extraction of extracellular polymers from activated sludge using a cation exchange resin. *Water research*, *30*(8), 1749-1758.

[34] Decremps, S. (2014). *Caractérisation du résidu particulaire et étude des mécanismes limitant la biodégradation des boues d'épuration* (Doctoral dissertation, Toulouse, INSA).

 [35] Box, J. D. (1983). Investigation of the Folin-Ciocalteau phenol reagent for the determination of polyphenolic substances in natural waters. *Water research*, *17*(5), 511-525.

[36] Gruskovnjak, A., Lothenbach, B., Holzer, L., Figi, R., & Winnefeld, F. (2006). Hydration of alkali-activated slag: comparison with ordinary Portland cement. *Advances in cement research*, *18*(3), 119-128.

[37] Vollpracht, A., Lothenbach, B., Snellings, R., & Haufe, J. (2016). The pore solution of blended cements: a review. *Materials and Structures*, *49*(8), 3341-3367.

[38] Puertas, F., Fernández-Jiménez, A., & Blanco-Varela, M. T. (2004). Pore solution in alkali-activated slag cement pastes. Relation to the composition and structure of calcium silicate hydrate. *Cement and Concrete Research*, *34*(1), 139-148.

[39] Myers, R. J., Bernal, S. A., & Provis, J. L. (2017). Phase diagrams for alkali-activated slag binders. *Cement and Concrete Research*, *95*, 30-38.

[40] Haha, M. B., Le Saout, G., Winnefeld, F., & Lothenbach, B. (2011). Influence of activator type on hydration kinetics, hydrate assemblage and microstructural development of alkali activated blast-furnace slags. *Cement and Concrete Research*, *41*(3), 301-310.

[41] Wang, S. D., & Scrivener, K. L. (1995). Hydration products of alkali activated slag cement. *Cement and Concrete Research*, *25*(3), 561-571.

[42] Tipping, E. (2002). *Cation binding by humic substances* (Vol. 12). Cambridge University Press.

[43] Santos, A. M., Bertoli, A. C., Borges, A. C. C., Gomes, R. A., Garcia, J. S., & Trevisan, M. G. (2018). New Organomineral Complex from Humic Substances Extracted from Poultry Wastes: Synthesis, Characterization and Controlled Release Study. *Journal of the Brazilian Chemical Society*, *29*(1), 140-150.

[44] Stevenson, F. J., & Goh, K. M. (1971). Infrared spectra of humic acids and related substances. *Geochimica et Cosmochimica Acta*, *35*(5), 471-483.

[45] Naithani, V., Singh, A. P., & Nautiyal, M. K. (2017). Spectroscopic Characterization of Humic Acids Extracted From Different Type of Soils of Punjab. *Journal of the Indian Society of Soil Science*, *65*(1), 24-31.

[46] Cao, P., Yao, J., Ren, B., Gu, R., & Tian, Z. (2002). Surface-enhanced Raman scattering spectra of Thiourea adsorbed at an iron electrode in NaClO4 solution. *The Journal of Physical Chemistry B*, *106*(39), 10150-10156.

[47] Clare, K. E., & Sherwood, P. T. (1954). The effect of organic matter on the setting of soilcement mixtures. *Journal of Applied Chemistry*, *4*(11), 625-630.

[48] de Souza, F., & Bragança, S. R. (2018). Extraction and characterization of humic acid from coal for the application as dispersant of ceramic powders. *Journal of Materials Research and Technology*, *7*(3), 254-260.

[49] Gin, S., Godon, N., Mestre, J. P., Vernaz, E. Y., & Beaufort, D. (1993). Experimental investigation of aqueous corrosion of R7T7 nuclear glass at 90°C in the presence of humic acids: A kinetic approach. *MRS Online Proceedings Library Archive*, *333*.

[50] Paul, S., Sharma, T., Saikia, D., Saikia, P., Borah, D., & Baruah, M. (2015). Evaluation of pKa values of soil humic acids and their complexation properties. *Int. J. Plant Soil Sci*, *6*(4), 218-228.

[51] Struyk, Z., & Sposito, G. (2001). Redox properties of standard humic acids. *Geoderma*, *102*(3-4), 329-346.

[52] Pokrovski, G. S., & Schott, J. (1998). Experimental study of the complexation of silicon and germanium with aqueous organic species: implications for germanium and silicon transport and Ge/Si ratio in natural waters. *Geochimica et Cosmochimica Acta*, *62*(21-22), 3413-3428.

[53] Prietzel, J., Thieme, J., Salomé, M., & Knicker, H. (2007). Sulfur K-edge XANES spectroscopy reveals differences in sulfur speciation of bulk soils, humic acid, fulvic acid, and particle size separates. *Soil Biology and Biochemistry*, *39*(4), 877-890.

[54] Casagrande, D. J., Gronli, K., & Sutton, N. (1980). The distribution of sulfur and organic matter in various fractions of peat: origins of sulfur in coal. *Geochimica et Cosmochimica Acta*, *44*(1), 25-32.

[55] Chen, H., & Wang, Q. (2006). The behaviour of organic matter in the process of soft soil stabilization using cement. *Bulletin of Engineering Geology and the Environment*, *65*(4), 445-448.

[56] Santosa, S. J., & Kunarti, E. S. (2008). Synthesis and utilization of Mg/Al hydrotalcite for removing dissolved humic acid. *Applied Surface Science*, *254*(23), 7612-7617.

[57] Swift, R. S., & Posner, A. M. (1972). Autoxidation of humic acid under alkaline conditions. *Journal of Soil Science*, *23*(4), 381-393.

[58] Provis, J. L., & Van Deventer, J. S. (Eds.). (2013). *Alkali activated materials: state-of-the-art report, RILEM TC 224-AAM*(Vol. 13). Springer Science & Business Media.